

Joint Optimization of Data- and Model-Driven Probing Beams and Beam Predictor

Tianheng Lu, Fan Meng, Zhilei Zhang, Yongming Huang, *Senior Member, IEEE*,
Cheng Zhang, *Member, IEEE*, Xiaoyu Bai

Abstract—Hierarchical search in millimeter-wave (mmWave) communications incurs significant beam training overhead and delay, especially in a dynamic environment. Deep learning-enabled beam prediction is promising to significantly mitigate the overhead and delay, efficiently utilizing the site-specific channel prior. In this work, we propose to jointly optimize a data- and model-driven probe beam module and a cascaded data-driven beam predictor, with limitations in that the probe and communicate beams are restricted within the manifold space of uniform planer array and quantization of the phase modulator. First, The probe beam module senses the mmWave channel with a complex-valued neural network and outputs the counterpart RSRPs of probe beams. Second, the beam predictor estimates the RSRPs in the entire beamspace to minimize the prediction cross entropy and selects the optimal beam with the maximum RSRP value for data transmission. Additionally, we propose to add noise to the phase variables in the probe beam module, against quantization error. Simulation results show the effectiveness of our proposed scheme.

Index Terms—mmWave communication, beam prediction, probing beam training, deep learning, data- and model-driven

I. INTRODUCTION

WITH sufficient bandwidth and potentially high data rates in B5G/6G communications [1], millimeter-wave (mmWave) communication technology has become a hot topic of research [2]. High-frequency signals suffer significant attenuation in propagation, and large-scale antenna arrays with beamforming is introduced to compensate for the path loss and simultaneously improve anti-interference capability [3]. However, the traditional hierarchical beam alignment/tracking (BA/T) incurs a large training overhead, resulting in inefficient beam training. Therefore, a low overhead and stable beam training method should be proposed urgently.

Conventional model-driven beam alignment schemes include exhaustive and hierarchical searches [4], which are unable to utilize the a priori knowledge of the channel state information (CSI) and have drawbacks such as high overhead and error propagation. In contrast, deep learning-based

schemes can effectively extract the CSI prior in temporal, frequency, and spatial domains to improve the prediction performance [5]–[8].

Many studies have focused on the design of beam predictors, e.g., [9], [10], and their idea can be summarized as using deep neural networks to find the mapping of a certain measured quantity to the optimal beam. Compared to traditional schemes, they improve the accuracy while reducing the interpretability and generalization of the model. The researchers in [11] jointly consider beam width design and power allocation strategy, but this scheme is difficult to obtain the global optimal solution, directly. Reference [10] learns a set of probe codebooks for a specific scenario, and it can be seen through simulation that the learned probe codebooks perform better than the wide beam. However, the method has more training parameters, especially when the ULA antenna is extended into a UPA antenna.

In this work, we predict the optimal beam in beamspace with RSRPs of a small number of probe beams. The principle of beam prediction is to utilize the airspace beam correlation to realize nonlinear interpolation, and the performance of beam prediction is mainly affected by two aspects: the probe beams and the beam predictor. We take beam prediction performance as optimization objective, and the probe beams and the beam predictor as the optimization variables, to achieve low beam training overhead and approximate the optimal intelligent real-time BA/T performance. The main contributions are summarized as follows.

1) *Data- and model-driven Probing Beam Training*: To compensate for the lack of physical understanding and poor generalization ability of traditional pure data-driven schemes, we propose a complex-value neural network (CVNN) that employs DFT-like manifold to generate probe beams in the training process. CVNN has the advantages of fewer training parameters and better generalization ability, which can effectively extract the features of the mmWave propagation environment and empower the downstream prediction task.

2) *Beam Domain Equivalent Variables*: We propose to train the CVNN with equivalent variables of the horizontal and vertical angles, i.e., the variables in beamspace. The angle-based beams only cover a small beamspace and the counterpart gradient is not smooth w.r.t. the angle variables. While, the beam-based variables cover the entire beamspace and have a smooth gradient, leading to better beam prediction accuracy.

3) *Noise Adding Technique*: Considering the limited phase resolution of practical mmWave devices, the learned probe beams have significant performance degradation after phase

This work was supported in part by the National Key R&D Program of China under Grant 2020YFB1806600 and the National Natural Science Foundation of China under Grant No. 62225107, 62001103 and 62201394, and the Fundamental Research Funds for the Central Universities under Grant 2242022k60002.

T. Lu, F. Meng, Z. Zhang, X. Bai, C. Zhang and Y. Huang are with the Purple Mountain Laboratories, Nanjing 211111, China (e-mail: th_lu@seu.edu.cn; mengfan@pmlabs.com.cn; zhangzhilei@pmlabs.com.cn; baixiaoyu@pmlabs.com.cn; zhangcheng_seu@seu.edu.cn; huangym@seu.edu.cn). C. Zhang and Y. Huang are (also) with the National Mobile Communications Research Laboratory, School of Information Science and Engineering, Southeast University, Nanjing 210096, China.

quantization. To address this issue, we propose additional noise on the phases of probe beams during training, to simulate quantization operation.

Notations: Lower-case and upper-case boldface letters \mathbf{a} and \mathbf{A} denote a vector and a matrix, respectively; \mathbf{A}^H and \mathbf{A}^T denote the conjugate transpose and transpose of matrix \mathbf{A} ; $|\cdot|$, \otimes respectively denote absolute and Kronecker product operators. $\mathbb{E}\{\cdot\}$, \mathbb{R} , \mathbb{C} represent the expectation, real and complex fields.

II. SYSTEM MODEL AND PROBLEM FORMULATION

A. System Model

Consider a link-level downlink mmWave multiple-input single-output (MISO) communication system consisting of a single base station (BS) and a mobile user (MU). The BS is equipped with a large uniform planar array (UPA) where N antennas are connected to a radio frequency (RF) chain, and the MU has an isotropic antenna. The BS uses the codewords in a DFT codebook $\mathcal{A} = \{\mathbf{a}_i\}_{i=1}^N$ where $\mathbf{a}_i \in \mathbb{C}^{N \times 1}, \forall i$, to probe the channel and communicate with the MU. Based on the 3GPP channel modeling, the downlink channel $\mathbf{h} \in \mathbb{C}^{N \times 1}$ is characterized as a superposition of M -paths propagation due to interactions (reflections, diffractions, penetrations, scattering) at stationary obstacles (hills, buildings, towers) and mobile objects (cars, pedestrians), given as

$$\mathbf{h} = \sum_{m=1}^M \alpha_m \psi(\phi_m, \theta_m), \quad (1)$$

where α is the complex gain coefficient, ϕ and θ respectively are the horizontal and vertical angles, and the UPA response ψ is expressed as

$$\psi(\phi, \theta) = \mathbf{a}_{xy}(\phi, \theta) \otimes \mathbf{a}_z(\theta), \quad (2)$$

where

$$\mathbf{a}_{xy}(\phi, \theta) = \frac{1}{\sqrt{N_\phi}} [1, e^{j\pi \sin \phi \sin \theta}, \dots, e^{j\pi(N_\phi-1) \sin \phi \sin \theta}]^T, \quad (3)$$

$$\mathbf{a}_z(\theta) = \frac{1}{\sqrt{N_\theta}} [1, e^{j\pi \cos \theta}, \dots, e^{j\pi(N_\theta-1) \cos \theta}]^T, \quad (4)$$

where N_ϕ and N_θ represent the number of antennas in the horizontal and vertical directions of the array, respectively, and $N = N_\theta \times N_\phi$ is the total number of antennas.

B. Problem Formulation

In a beam alignment process, the BS first transmits beams in a probe beam codebook to sense the downlink channel. The probe beam codebook \mathbf{W} is composed of L probe beams, and $\mathbf{W} = [\mathbf{w}_1, \dots, \mathbf{w}_L]$ where $\mathbf{w}_l \in \mathcal{A}, \forall l \in \{1, \dots, L\} = \mathcal{L}$. Then, the MU receives the probe signals and feedbacks the counterpart RSRPs to the BS. It has to be noticed that the transmitting and feedback should all be finished in the same channel coherence time. The l -the entry of the MU's feedback RSRPs $\mathbf{z} = [z_1, \dots, z_L]^T$ is written as

$$z_l = \sqrt{P} \mathbf{h}^H \mathbf{w}_l s + n_l, \forall l \in \mathcal{L}, \quad (5)$$

where P is BS transmit power, s is baseband signal with unit power, and n_l is additive white gaussian noise. We denote receive signal power as $\mathbf{x} = |\mathbf{z}|^2$, and \mathbf{x} is further quantized as RSRPs \mathbf{x}_q by a map g . Using RSRPs \mathbf{x}_q as input, the BS learns to infer the optimal transmit beam in the DFT codebook by a learnable map $f : \mathbf{x}_q \rightarrow i^*$. Moreover, the probe beam codebook is parameterized by learnable parameters $\{\phi_l, \theta_l\}_{l=1}^L$. Finally, the joint optimization problem of data- and model-driven probing beams and beam predictor is expressed as follows

$$\min_{\theta, \phi, f} \mathbb{E}_{\mathbf{h}, \mathbf{n}} \{d(\hat{\mathbf{y}}, \mathbf{y}^{\text{tar}})\} \quad (6a)$$

$$\mathbf{W} = \psi(\theta, \phi), \quad (6b)$$

$$\theta_j \in [0, \pi], \forall l \in \mathcal{L}, \quad (6c)$$

$$\phi_j \in [-\frac{\pi}{2}, +\frac{\pi}{2}], \forall l \in \mathcal{L}, \quad (6d)$$

$$(5),$$

$$\mathbf{x}_q = g(|\mathbf{z}|^2), \quad (6e)$$

$$\hat{\mathbf{y}} = f(\mathbf{x}_q), \quad (6f)$$

$$\hat{i}^* = \arg \max \hat{\mathbf{y}}, \quad (6g)$$

where d is a distance function, \mathbf{y}^{tar} is the target of the beam predictor. Map g converts the received signal into RSRP, i.e., $g : \max(\min(10 \log_{10}(\cdot), -40), -140)$, indicating the RSRP is capped between -140 to -40 dBm. Particularly, the RSRP is not quantized during training and is quantized with 1 dBm resolution for online inference.

III. DATA- AND MODEL-DRIVEN SOLUTION OF PROBE BEAM TRAINING AND BEAM PREDICTOR

As shown in Fig. 1, the overall learning problem (6) is composed of a probe beam training module with θ, ϕ , and a cascaded beam predictor with f , and we discuss the counterpart solution. In general, the probe codebook and the beam predictor are parameterized with separate neural networks and jointly trained in an end-to-end manner, via the stochastic gradient descent method. In this way, the probe beams are indirectly optimized to assist in the downstream prediction effort.

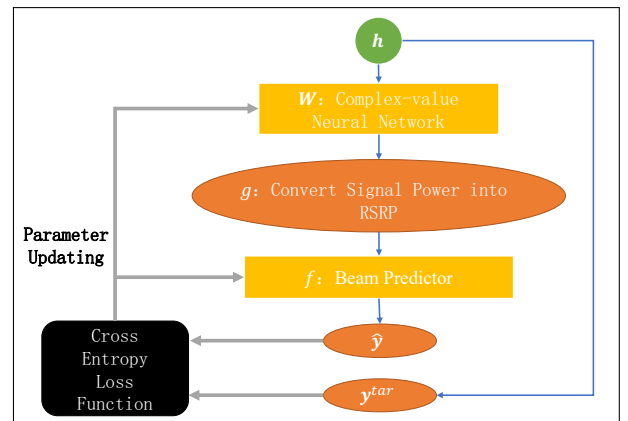


Fig. 1: The illustrative procedure of the proposed scheme.

A. Probe Beam Training

We propose to design the probe beam training module with a complex-valued neural network (CVNN), and derive the output gradient w.r.t. the learnable parameters θ, ϕ .

To directly characterize the energy magnitude and at the same time facilitate the computation, we take $\mathbf{z} = [(x_1^r)^2 + (x_1^i)^2, \dots, (x_L^r)^2 + (x_L^i)^2]^T$ as an input to the subsequent multi-classifier. Denote the loss function as J , according to the derived chain rule, the partial gradient w.r.t. ϕ_j is expressed as

$$\frac{\partial J}{\partial \phi_j} = \frac{\partial J}{\partial |z_j|^2} \frac{\partial |z_j|^2}{\partial z_j} \frac{\partial z_j}{\partial \phi_j}, \quad (7)$$

where $\frac{\partial J}{\partial |z_j|^2}$ can be derived by automatic differentiation with Pytorch in implementation. Although $|z_j|^2$ is not complex differentiable w.r.t. z_j , its gradient can be computed by treating the real and imaginary parts of z_j separately: $\frac{\partial |z_j|^2}{\partial z_j} = [2z_j^r, 2z_j^i]$. And the expression of $\frac{\partial z_j}{\partial \phi_j}$ is written as

$$\frac{\partial z_j}{\partial \phi_j} = \begin{bmatrix} \frac{\partial z_j^r}{\partial \phi_j} \\ \frac{\partial z_j^i}{\partial \phi_j} \end{bmatrix} = \begin{bmatrix} \sum_{n=1}^N \left(\frac{\partial w_{jn}^r}{\partial \phi_j} h_n^r - \frac{\partial w_{jn}^i}{\partial \phi_j} h_n^i \right) \\ \sum_{n=1}^N \left(\frac{\partial w_{jn}^r}{\partial \phi_j} h_n^i + \frac{\partial w_{jn}^i}{\partial \phi_j} h_n^r \right) \end{bmatrix}, \quad (8)$$

where

$$\begin{aligned} \frac{\partial w_{jn}^r}{\partial \phi_j} &= \frac{1}{\sqrt{N}} \left\{ -\sin\{\pi[(\lceil \frac{n}{N_\theta} \rceil - 1) \sin \phi_j \sin \theta_j \right. \\ &\quad \left. + (n - \lceil \frac{n}{N_\theta} \rceil N_\theta + N_\theta - 1) \cos \theta_j]\} \right\} \\ &\quad \cdot \pi[(\lceil \frac{n}{N_\theta} \rceil - 1) \sin \theta_j \cos \phi_j], \end{aligned} \quad (9a)$$

$$\begin{aligned} \frac{\partial w_{jn}^i}{\partial \phi_j} &= \frac{1}{\sqrt{N}} \left\{ \cos\{\pi[(\lceil \frac{n}{N_\theta} \rceil - 1) \sin \phi_j \sin \theta_j \right. \\ &\quad \left. + (n - \lceil \frac{n}{N_\theta} \rceil N_\theta + N_\theta - 1) \cos \theta_j]\} \right\} \\ &\quad \cdot \pi[(\lceil \frac{n}{N_\theta} \rceil - 1) \sin \theta_j \cos \phi_j]. \end{aligned} \quad (9b)$$

Similarly, for the update of θ_j ,

$$\frac{z_j}{\partial \theta_j} = \begin{bmatrix} \frac{z_j^r}{\partial \theta_j} \\ \frac{z_j^i}{\partial \theta_j} \end{bmatrix} = \begin{bmatrix} \sum_{n=1}^N \left(\frac{\partial w_{jn}^r}{\partial \theta_j} h_n^r - \frac{\partial w_{jn}^i}{\partial \theta_j} h_n^i \right) \\ \sum_{n=1}^N \left(\frac{\partial w_{jn}^r}{\partial \theta_j} h_n^i + \frac{\partial w_{jn}^i}{\partial \theta_j} h_n^r \right) \end{bmatrix}, \quad (10)$$

where

$$\begin{aligned} \frac{\partial w_{jn}^r}{\partial \theta_j} &= \frac{1}{\sqrt{N}} \left\{ -\sin\{\pi[(\lceil \frac{n}{N_\theta} \rceil - 1) \sin \phi_j \sin \theta_j \right. \\ &\quad \left. + (n - \lceil \frac{n}{N_\theta} \rceil N_\theta + N_\theta - 1) \cos \theta_j]\} \right\} \\ &\quad \cdot \pi[(\lceil \frac{n}{N_\theta} \rceil - 1) \sin \phi_j \cos \theta_j \\ &\quad - (n - \lceil \frac{n}{N_\theta} \rceil N_\theta + N_\theta - 1) \sin \theta_j], \end{aligned} \quad (11a)$$

$$\begin{aligned} \frac{\partial w_{jn}^i}{\partial \theta_j} &= \frac{1}{\sqrt{N}} \left\{ \cos\{\pi[(\lceil \frac{n}{N_\theta} \rceil - 1) \sin \phi_j \sin \theta_j \right. \\ &\quad \left. + (n - \lceil \frac{n}{N_\theta} \rceil N_\theta + N_\theta - 1) \cos \theta_j]\} \right\} \\ &\quad \cdot \pi[(\lceil \frac{n}{N_\theta} \rceil - 1) \sin \phi_j \cos \theta_j \\ &\quad - (n - \lceil \frac{n}{N_\theta} \rceil N_\theta + N_\theta - 1) \sin \theta_j]. \end{aligned} \quad (11b)$$

After offline training, the parameters of the probe beams are further quantized for online deployment.

B. Beam Predictor

The beam predictor infers the beam with maximum RSRP value by extracting the prior information implicitly embedded in the CSI dataset that reflects the site-specific propagation environment. After the CVNN outputs the power \mathbf{z} of the probe beams and quantized by the map g , the RSRPs \mathbf{x}_q is fed into the beam predictor which is enabled by a deep neural network (DNN). The DNN output is the distribution of the optimal beam in the entire DFT space, i.e., $\hat{\mathbf{y}} \in \mathbb{R}^{N \times 1}$. The optimal beam, i.e., $i^* = \arg \max \hat{\mathbf{y}}$, is selected as the communication beam. We use cross entropy as the distance function, so the activation function of the output layer is softmax: $\sigma(z_i) = \frac{e^{z_i}}{\sum_{j=1}^N e^{z_j}}$, $i = \{1, \dots, N\}$, and the target label \mathbf{y}^{tar} is a one-hot vector.

Through the output layer, we can either directly get the predicted optimal beam, or for the consideration of robustness, re-probe the Top- K beams with the largest probabilities. Then the beam with the highest RSRP is regarded as the optimal beam, whose procedure is similar to the two-level search in 3GPP, but the searching space is greatly reduced with our proposed scheme.

C. Probe Beam Training with Beamspace Variables

At the initial stage of the study, our scheme treats the horizontal angle ϕ and vertical angle θ of the probe beam as a set of trainable parameters, to generate DFT-like beams. However, the beam prediction accuracy is not significantly improved. In fact, the angle-based representation of beams is restricted in the range $[-60, 60]^\circ$, and the beam width is angle-related. For example, the beam around 0° is thinner than the beam around $\pm 60^\circ$. This indicates the loss gradient is not smooth w.r.t. horizontal-vertical angles, resulting in difficulties during training.

To enlarge the probe range, we propose to use the equivalent variables $u = \sin \phi \sin \theta$ and $v = \cos \theta$ in the beam domain (both in range $[-1, 1]$) instead of the angle domain (in range $[-\pi/2, \pi/2]$), to design the learnable probe beams. Moreover, the loss gradient is uniform w.r.t. the beam-domain variables u, v .

D. Phase Quantization

In practical deployment, the analog precoders usually have limited phase resolution B , such as 3–7 bits. During training, the effects of phase quantization are not considered, since back-propagation can be ruined by the quantization operations. However, the learned model can be not robust to the quantizations, to simulate the effects of phase quantization. To address this issue, we propose to add noise to the phases during training. Particularly, the additional noise follows uniform distribution in range $[-1/2^B, 1/2^B]^\circ$.

In summary, the data- and model-driven probe beam training and beam predictor takes channel \mathbf{h} as inputs and optimizes learnable probe beams during the training phase, whose

Algorithm 1: Data-Driven Beam Predictor (online inference)

- 1 **Initialize:** learned probe codebook \mathbf{W} after quantization, learned beam predictor f ;
Output: communication beam \mathbf{w}_{i^*} .
 - 2 The BS senses the downlink channel with \mathbf{W} ;
 - 3 The UE feedbacks the counterpart RSRPs to the predictor f at the BS side;
 - 4 The BS selects and re-probes the top-5 beams, then gets the counterpart RSRPs;
 - 5 The BS selects the beam with maximum RSRP for data transmission, i.e., \mathbf{w}_{i^*} .
-

mathematical form naturally has DFT-like manifold. In the deployment phase, the parameters of the probe beams are further quantized by the phase resolution of analog devices. The online inference process is demonstrated in Algorithm 1.

IV. SIMULATIONS

A. Configurations

To evaluate the performance of our proposed data- and model-driven scheme, the mmWave channel is established as a map-based deterministic model according to 3GPP 38.901 [12], and stochastic clusters are also introduced. The DNN-based beam predictor consists of one input layer, three hidden layers, and one output layer. Scenario-related details and the specific configuration of the DNN are summarized in Table I and Table II, respectively.

TABLE I: Simulation Configurations of Scenario

Name	Value
BS antenna number	16×8
MU antenna number	1
Carrier frequency f_c	30 GHz
Bandwidth B	100 MHz
noise power spectral density	-174 dBm/Hz
probing beam number L	8
symbol duration T_s	8.92 μ s
time-slot duration T_c	20 ms

TABLE II: Configurations of DNN

Name	Value
Input layer nodes number	8
Hidden layer 1 nodes number	200
Activation function 1	LeakyReLU(0.04)
Hidden layer 2 nodes number	200
Activation function 2	LeakyReLU(0.04)
Hidden layer 3 nodes number	200
Activation function 3	ReLU
Output layer nodes number	128

For performance validation, two metrics are considered:
 1) Top- K beam prediction accuracy, the probability that the optimal beam appears in the top K predicted beams (sorted by

predicted RSRP). 2) Effective achievable rate (EAR), which is defined as

$$\text{EAR} \triangleq \mathbb{E}_{\mathbf{h}, \mathbf{n}_x} \left\{ \left(1 - \frac{LT_s}{T_c} \right) \log_2 \left(1 + \frac{|\mathbf{A}[:, i^*] \mathbf{h}|^2}{\sigma_x^2} \right) \right\}, \quad (12)$$

where T_s and T_c respectively are the durations of a symbol and a time slot.

The *baseline* scheme uniformly chooses probe beams from the DFT codebook on the beamspace. The reference scheme [10] treats all elements in \mathbf{W} as learnable parameters with constant modulus constraint. The whole end-to-end network uses the cross-entropy function as the loss function and is trained for 200 epochs using the Adam optimizer on the simulation platforms: Python 3.8.13, Pytorch 1.10.2.

B. Training Convergence Speed

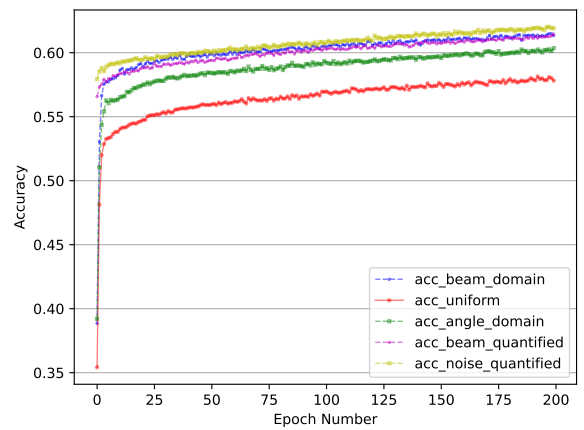


Fig. 2: The top-3 prediction accuracy versus training epoch.

This subsection focuses on the training convergence speed. In Fig. 2, the uniform probe beam scheme performs poorly, and even after 200 epochs of training, it only obtains an accuracy rate equivalent to 10 epochs of the proposed schemes. While the training speed of our proposed schemes is faster, the beam domain scheme has an obvious speed gain compared with the angle domain scheme. In addition, when quantization noise is taken into account, the training speed of the proposed scheme can be greatly improved further.

C. Top- K Beam Prediction Accuracy

After training, the results evaluated by Top- K beam prediction accuracy are investigated, where $K \in \{1, 3, 5\}$.

In Fig. 3, the *baseline* scheme is not satisfactory, but we can initialize the proposed trainable probe beams with the uniform probe codebook. With regard to the remaining schemes, angle_domain scheme directly uses horizontal and vertical angles $\{\phi, \theta\}$ as training parameters, while beam_domain uses $\{u, v\}$ for training. The two schemes are theoretically equivalent, but in practice, it can be found that the scheme with beam-based variables achieves higher accuracy. Besides, we find that the phase quantization of the probe beams seriously degrades the performance, that is, the probe beams are sensitive to the quantization noise. To solve this problem, we propose adding

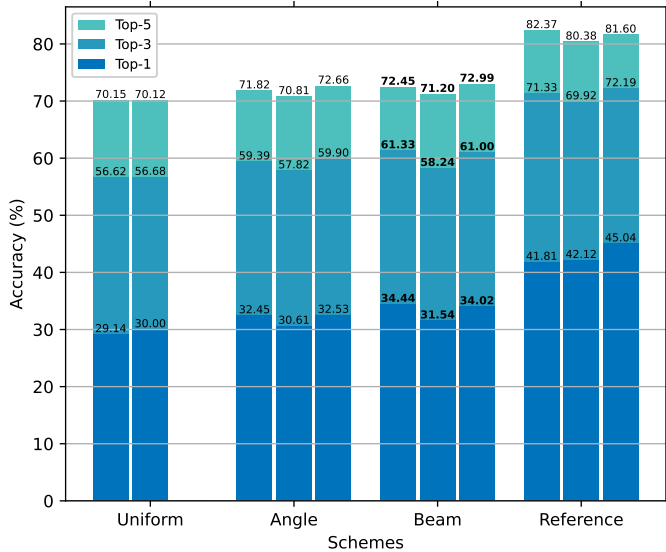


Fig. 3: Top- K beam prediction accuracy for different schemes. In each scheme, from left to right are the original scheme, quantization scheme and noise scheme, respectively.

uniform noise on the phases in the training process, and noise adding significantly improves the prediction accuracies on all schemes, including the reference.

D. Effective Achievable Rate

Fig. 4 represents the trend of EAR with the number of users at a constant SNR. The two schemes for comparison are the binary search scheme and hierarchical search scheme. Consider a single user, the hierarchical search scheme needs 16 wide beams and 8 narrow beams while the binary search scheme requires $\log_2 128 = 8$ rounds of interaction, and the EAR performers of each scheme are close. With the number of users increasing, the performance of the search-based scheme deteriorates rapidly. When the user number reaches 100, the search time of the binary search scheme occupies all the channel coherence time and the corresponding EAR is 0. The hierarchical search scheme spends 60% of the time on searching for the best beam. In contrast, The prediction-based schemes achieve a 35% savings in training overhead, and performance remains high.

V. CONCLUSION

In this work, we studied the problem of data- and model-driven probe beam training and beam prediction, and utilized deep learning techniques to jointly optimize two networks in an end-to-end way. We also proposed equivalent beamspace variables to train the probe beam module and the noise-adding technology against phase quantization. Simulation results verified the effectiveness of the proposed methods. In future research, we will further extract the channel prior in both frequency and temporal domains via deep learning.

REFERENCES

[1] M. Xiao, S. Mumtaz, Y. Huang, L. Dai, Y. Li, M. Matthaiou, G. K. Karagiannidis, E. Björnson, K. Yang, C.-L. I, and A. Ghosh, "Millimeter wave communications for future mobile networks," *IEEE J. Sel. Areas Commun.*, vol. 35, no. 9, pp. 1909–1935, 2017.

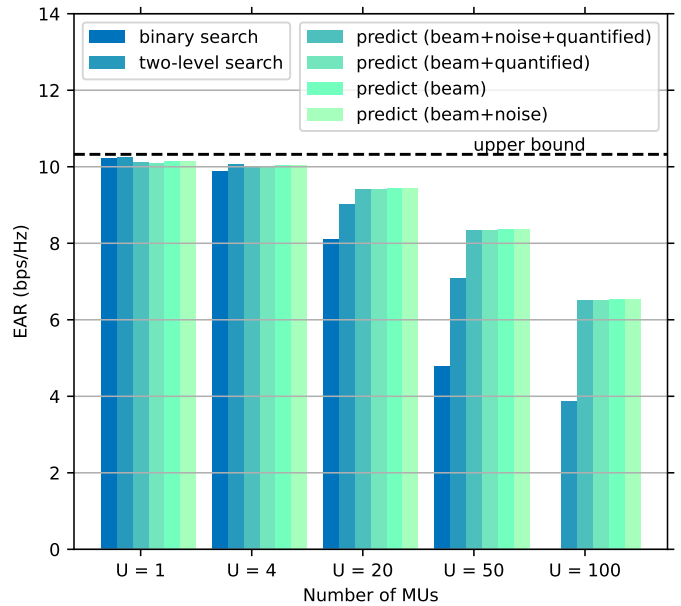


Fig. 4: EAR versus MU number.

[2] L. Li, D. Wang, X. Niu, Y. Chai, L. Chen, L. He, X. Wu, F. Zheng, T. Cui, and X. You, "mmwave communications for 5g: implementation challenges and advances," *Sci. China Inf. Sci.*, vol. 61, no. 2, p. 021301, 2018.

[3] S. Han, C.-l. I, Z. Xu, and C. Rowell, "Large-scale antenna systems with hybrid analog and digital beamforming for millimeter wave 5g," *IEEE Commun. Mag.*, vol. 53, no. 1, pp. 186–194, 2015.

[4] S. Hur, T. Kim, D. J. Love, J. V. Krogmeier, T. A. Thomas, and A. Ghosh, "Millimeter wave beamforming for wireless backhaul and access in small cell networks," *IEEE Trans. Commun.*, vol. 61, no. 10, pp. 4391–4403, 2013.

[5] R. Yang, Z. Zhang, X. Zhang, C. Li, Y. Huang, and L. Yang, "Meta-learning for beam prediction in a dual-band communication system," *IEEE Trans. Commun.*, vol. 71, no. 1, pp. 145–157, 2023.

[6] F. Meng, S. Liu, Y. Huang, and Z. Lu, "Learning-aided beam prediction in mmWave MU-MIMO systems for high-speed railway," *IEEE Trans. Commun.*, vol. 70, no. 1, pp. 693–706, 2022.

[7] J. Zhang, Y. Huang, J. Wang, X. You, and C. Masouros, "Intelligent interactive beam training for millimeter wave communications," *IEEE Trans. Wireless Commun.*, vol. 20, no. 3, pp. 2034–2048, 2021.

[8] K. Ma, F. Zhang, W. Tian, and Z. Wang, "Continuous-time mmwave beam prediction with ode-lstm learning architecture," *IEEE Wireless Commun. Lett.*, vol. 12, no. 1, pp. 187–191, 2023.

[9] W. Xu, F. Gao, S. Jin, and A. Alkhateeb, "3D scene-based beam selection for mmWave communications," *IEEE Wireless Commun. Lett.*, vol. 9, no. 11, pp. 1850–1854, 2020.

[10] Y. Heng, J. Mo, and J. G. Andrews, "Learning site-specific probing beams for fast mmwave beam alignment," *IEEE Trans. Wireless Commun.*, vol. 21, no. 8, pp. 5785–5800, 2022.

[11] H. Shokri-Ghadikolaei, L. Gkatzikis, and C. Fischione, "Beam-searching and transmission scheduling in millimeter wave communications," in *2015 IEEE Int. Commun. Conf. (ICC)*, 2015, pp. 1292–1297.

[12] 3GPP, "Study on channel model for frequencies from 0.5 to 100 GHz," 3GPP TR 38.901, Jan. 2020, version 16.1.0.